JOURNAL OF MATERIALS SCIENCE 25 (1990) 3561–3565

Oxidation behaviour of mullite-SiC composites

M. I. OSENDI
Intituto Cerámica y Vidrio, CSIC, Arganda del Rey, Madrid, Spain

The oxidation kinetics of three mullite–SiC composites were studied. The materials were all processed with the same amount of SiC, 10% by volume; in two of the composites the second phase was added as whiskers, and in the third as powders. The sintered composites were exposed to high temperatures (1200 to 1500° C) during variable time periods (maximum 122 h) under the oxidizing furnace atmosphere. The nature of the reaction layer formed has been analysed specifying the oxidation rate constants for each composite. The influence on the bend strength of the composites for one of the isothermal oxidizing treatments has also been measured.

1. Introduction

The addition of SiC whiskers to ceramic matrices, specially alumina, has demonstrated its effectiveness as a toughening agent [1, 2]. This ability to reinforce has also been tested at elevated temperatures [3, 4]. A more discreet enhancement of the toughness of mullite due to the presence of SiC whiskers has also been reported [2, 5], although mullite–SiC composites have not been so widely studied. One important issue, not sufficiently addressed, concerning these types of composites is their vulnerability in oxidizing conditions [6, 7].

Here the influence of the nature of the second phase (whiskers or powders) on the oxidation kinetics of mullite–SiC composites is investigated.

2. Experimental procedures

The raw materials used were all commercial products: mullite powders (grade SA 193 CR, Baikowski International, North Carolina, USA); two different kind of SiC whiskers, SiC–w_a (Silar SC-9, Arco Metals, South Carolina, USA) and SiC–w_b (SCW # 1, Tateho Chemical Co., Japan); and SiC powders, SiC–p (Type 99%, Cerac Inc., Wisconsin, USA). The proportion of the second phase was kept constant to 10% by volume. Composite materials were obtained by a conventional powder-processing route [5]. Firstly, mullite powders were attrition milled for 2 h in a teflon-lined jar with high-purity alumina balls in isopropyl alcohol. The SiC whiskers, after acid washing and ultrasonic dispersion, were added to the mullite slurry and the milling process continued a further 2 h. In the case of the SiC–p, mullite and SiC particles were attrition milled together for 4 h. Next, the dried and mixed powders were isostatically pressed at 200 MPa. Finally, samples were sintered in a furnace with a graphite resistance, inside alumina crucibles which were covered with an alumina lid. The sintering temperature, $\approx 1750°$ C, was maintained for 3 h in a flowing N_2 atmosphere.

The oxidation experiments were conducted in an electrical furnace, with heating elements of $MoSi_2$, under the oxidizing laboratory atmosphere. For thermal treatments, the samples were machined into bars of dimensions $2 \times 3 \times 15\,mm^3$, placed inside the cool furnace over a mullite plaque and subjected to the programmed temperature, always following the same heating and cooling ramps ($1200°\,C\,h^{-1}$). The temperatures selected for the treatments were 1200, 1300, 1400 and 1500° C, with holding times of 50, 72 and 122 h. The samples were weighed before and after each treatment. Cross sections of the oxidized bars were polished to observe the extension of the reaction layer in an optical microscope provided with a phototube. The length of this region was directly measured over the optical photographs. X-ray diffraction analyses (XRD) of the scale in the treated samples were obtained.

Some selected samples were observed in the scanning electron microscope (SEM) and microanalyses (EDX) of the oxidized areas were also obtained.

Finally, the flexural strength (σ_f) was measured in two of the three composites, mullite + SiC–w_a and mullite + SiC–p, before and after exposure at 1300° C for 122 h. Machined bars of dimensions $2 \times 3 \times 30$ were tested in three-point bending using a 20 mm span and a constant displacement rate of $0.05\,mm\,min^{-1}$. The σ_f was obtained as a mean value over five bars.

3. Results and discussion

In Table I the main characteristics of the three sintered mullite–SiC composites are shown. After thermal exposure all the samples showed a small weight gain, in agreement with the oxidation reaction

$$3\,Al_2O_3 \cdot 2\,SiO_2 + SiC + \tfrac{3}{2}\,O_2 \rightarrow 3\,Al_2O_3 \cdot 2\,SiO_2 + SiO_2\,(l) + CO\,(g)$$

This reaction would imply a 5% weight gain for a total oxidation of the SiC present in the samples (10% by volume). A maximum weight gain around 1% was measured in the bars.

Composites were initially green, but after the thermal treatments they changed their colour. At the

0022-2461/90 $03.00 + .12

TABLE I Characteristics of the mullite–SiC materials

	Density (%)	Young's modulus (GPa)	Thermal exp. coef. ($10^{-6}\,^{\circ}C^{-1}$)	Particle size (μm)	Impurities 2nd ph. (%)
M + CSi–w_a	97	197	5.9	$M \approx 3$ $w_a \approx 5$–10*	Metal 0.8† O_2 1.2
M + CSi–w_t	98	231	5.0	$M \approx 3$ $w_t \approx 2$*	Metal 1.4† O_2 0.5
M + CSi–p	99	240	5.3	$M \approx 3$ $p \approx 2$	Total $\leqslant 1$

*Whiskers length.

†Mainly calcium, aluminium, manganese, magnesium, iron.

lower test temperatures (1200 and 1300° C), the samples showed a progressive darkening on the surface. Conversely, at higher temperatures (1400 and 1500° C) the surface of samples whitened. An example of the polished cross sections of oxidized samples can be seen in Fig. 1. The absence of SiC (white phase in the picture) in the oxide region is obvious, and the interface between the two areas (reacted/non reacted) is almost straight line.

In Fig. 2, the evolution of the scale as a function of time is plotted for the three composites. The length of this region seems to be lineal with the square root of time; therefore the composites have parabolic rate constants. Similar behaviour has been reported in SiC materials [8] and also in Al_2O_3–SiC and mullite–SiC composites obtained by hot pressing [6, 7]. In Table II, the parabolic rate constants of each composite at all the test temperatures are listed, together with results given in the literature for sintered α-SiC [8]. The parabolic rate constants (k) are 3 to 4 orders of magnitude greater in the composites than in the α-SiC at all the studied temperatures. Furthermore, the whisker composites have larger k than the particulate one, especially at 1200 and 1300° C (see Table II and

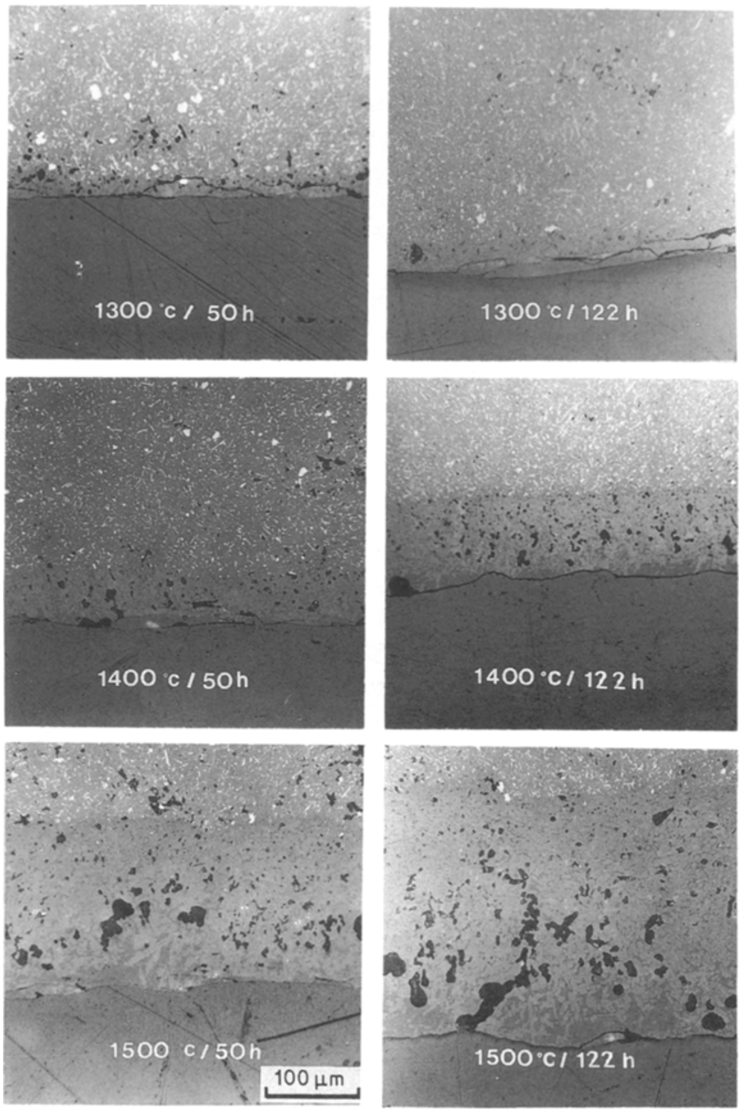

Figure 1 Optical micrographs of polished cross sections of the M + SiC–w_a samples, isothermally treated at the temperatures and times indicated.

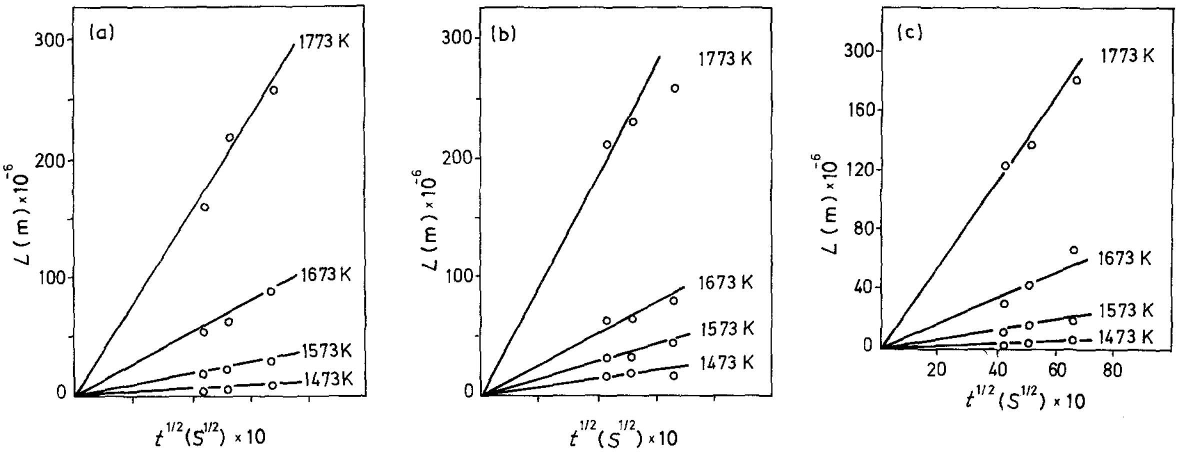

Figure 2 Extension of the oxidized scale as a function of the square root of time for the three mullite–SiC composites. (a) M + 10 vol % SiC–w_a; (b) M + 10 vol % SiC–w_t; (c) M + 10 vol % SiC–p.

Fig. 3). This could be a consequence of the lower porosity in the mullite + SiC–p composite (Table I), and lower porosity may make it more difficult for the oxygen in the atmosphere to reach the SiC phase.

In Fig. 3 the Arrhenius plots of the rate constants for the three composites are represented and the apparent activation energies obtained are listed in Table II. The M + SiC–w_t composite is the only one that has a change in behaviour between the low (1200 and 1300° C) and high (1400 and 1500° C) temperature regions. Costello and Tressler [8] have also observed this type of inflection point around 1400° C for SiC materials, which they attributed to a possible change in the rate-controlling mechanism of oxidation of SiC. The activation energies (Table II) ranged from 437 to 591 kJ mol^{-1}, whereas the M + SiC–w_t composite showed an activation energy of 279 kJ mol^{-1} in the low-temperature side (see Fig. 3). In general, the activation energies seem to be higher than those reported for the sintered α-SiC [8], and hot-pressed mullite–SiC [6, 7] composites with 20 to 30% by volume of the non oxide phase. Activation energies in the order of 100 to 150 kJ mol^{-1} have been attributed to the diffusion of molecular oxygen through the silica film [8] formed during oxidation. In the present case, the activation energies are much higher so the rate-controlling mechanism should be different. Furthermore, in these composites the oxide scale is not pure silica, as will be discussed later on.

The only crystalline phase found by XRD on the surface of the oxide samples was mullite, as expected. The other phase coexisting with mullite in this region is a glass as shown by the SEM micrographs of the oxidized region (see Fig. 4). The large pores observed in this figure are produced by gas evolution, according to Equation 1, through the reaction layer. The composition of the glass changed depending on the thermal treatment, but was always an aluminosilicate with alkaline impurities: Na_2O, CaO and K_2O, up to 5% by weight in some areas, according to the EDX micro-

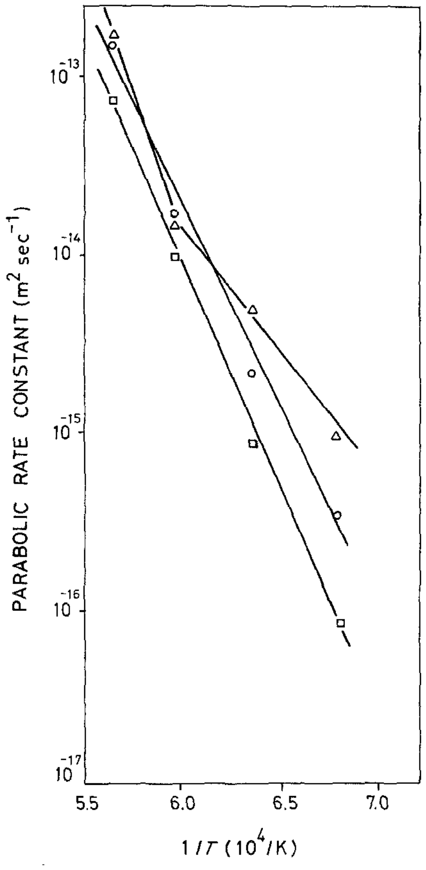

Figure 3 Arrhenius plot of the parabolic rate constants for the mullite–SiC composites. ○, M + SiC–w_a; △, M + SiC–w_t; □, M + SiC–p.

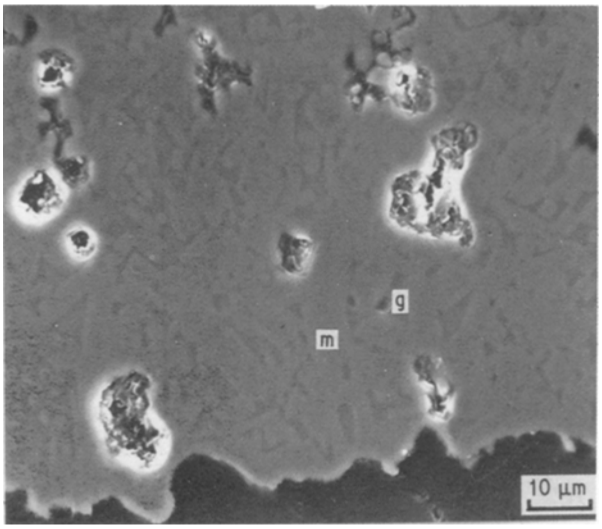

Figure 4 Cross-section SEM micrographs of the reaction layer for the composite M + SiC–p treated at 1500° C for 122 h. (M, Mullite; g, glassy phase).

TABLE II Parabolic rate constants (k)

T (K)	k ($m^2 sec^{-1}$)			
	M + $SiC\text{-}w_a$	M + $SiC\text{-}w_t$	M + SiC-p	α-SiC [7]
1473	3.5e(−16)	9.4e(−16)	0.8e(−16)	1.4e(−18)
1573	2.2e(−15)	4.9e(−15)	0.9e(−15)	2.9e(−18)
1673	1.8e(−14)	1.5e(−14)	1.0e(−14)	6.3e(−18)
1773	1.6e(−13)	1.7e(−13)	0.8e(−13)	3.1e(−17)
E_A ($kJ\,mol^{-1}$)	437	279–591	487	134–389

analyses. The impurity concentration is higher in the glass formed, which acts like an impurity sink, than in the mullite grains. The presence of these impurities would explain the existence of a liquid at much lower temperatures (such as 1200° C) than those predicted by the Al_2O_3–SiO_2 equilibrium phase diagram [9] that is around 1587° C. These impurities, especially the calcium, come mainly from the whiskers and, in the case of Na_2O and K_2O, are probably processing contaminants. They determine the nature (viscosity and composition) and amount of the liquid phase. As a result, the higher values of the rate constants (k) in the composite M + $SiC\text{-}w_t$ (see Table II) at the lower temperatures, could be attributed to the higher impurity level in these whiskers, as reflected in Table I.

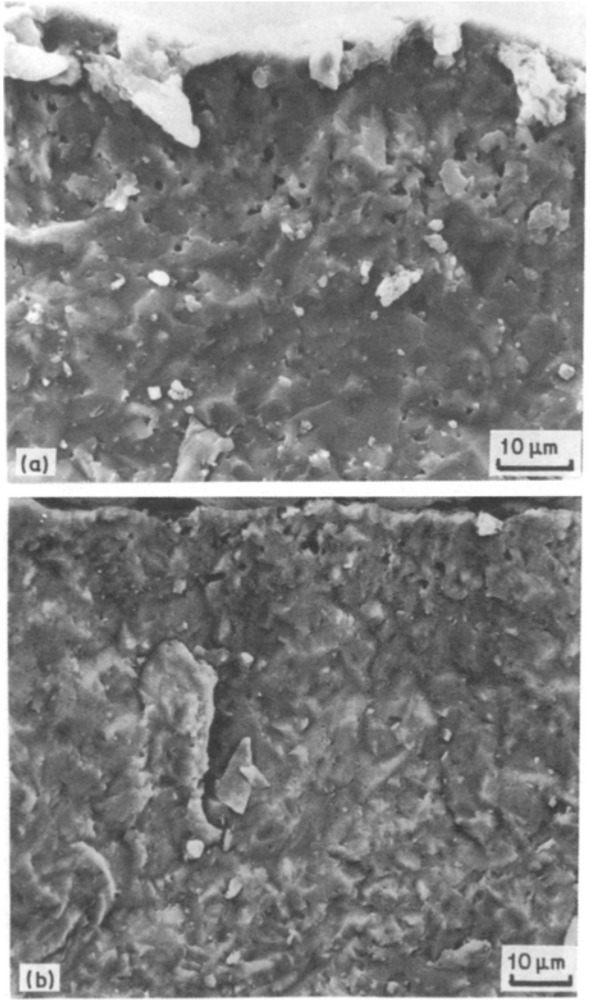

Figure 5 Fracture surfaces of (A) M + $SiC\text{-}w_a$ and (B) M + SiC-p composites after 122 h at 1300° C, showing an area close to one edge (see text).

Although the rate controlling mechanism for oxidation of composites of the type oxide matrix/SiC seems to be determined by the matrix material [6, 7], the differences among composites with the same matrix depends fundamentally on the impurities of the SiC phase.

In Table III the σ_f values for the M + $SiC\text{-}w_a$ and M + SiC-p composites, before and after a thermal treatment of 122 h at 1300° C, are shown. From the data, it seems that this treatment does not degrade the material. This could be due to the fact that the extension of the oxide scale in both composites is of the same order as the critical flaw size (~ 30 µm) calculated for those composites without thermal exposure [5]. Larger exposure times and higher temperatures would probably produce a decrease on the bend strengths. In Fig. 5, fracture surfaces of these materials are shown. In these micrographs the porosity layer underneath the external surface and the glassy areas are clearly observed. In Fig. 6, the gas entrapped by the amorphous phase could be observed as bubbles formed over the surface of samples. In this particular sample, the glass was probably of high viscosity.

To summarize, the three mullite-SiC composites (10 vol %) studied seem to have parabolic oxidation kinetics between 1200 and 1500° C, with rate constants 3 to 4 orders of magnitude higher than the SiC materials. The oxidation rate in the composites depends on the porosity and impurities existing on the samples. The rate-controlling mechanism is not yet clear in these kinds of composites. When samples were oxidized at 1300° C for 122 h, they did not show any decrease on the bend strengths.

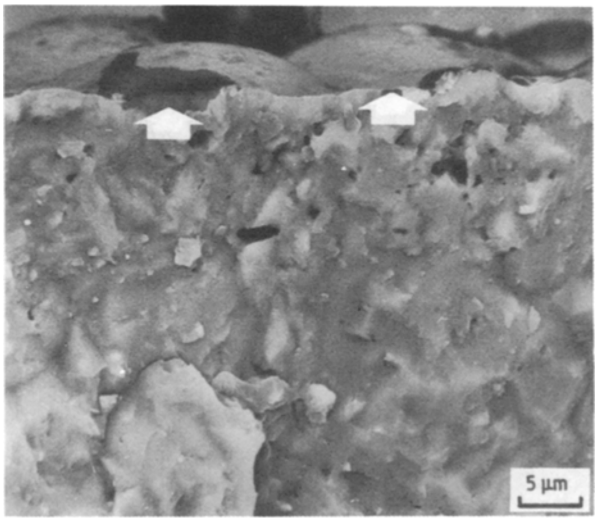

Figure 6 Back scattered electron micrograph of gas bubbles (arrows) formed on the surface of a M + $SiC\text{-}w_a$ composite bar after an oxidizing treatment (1300° C, 122 h).

TABLE III Flexural strengths on mullite–SiC composites

Material	σ_f (MPa)	
	As-sintered	After 122 h at 1300° C
M + SiC-w_a	247 ± 12	225 ± 23
M + SiC-p	262 ± 20	269 ± 22

References

1. G. C. WEI and P. F. BECHER, *Amer. Ceram. Soc. Bull.* **64** (1985) 298.
2. P. F. BECHER, C. H. HSUEH, P. ANGELINI and T. TIEGS, *J. Amer. Ceram. Soc.* **71** (1988) 1050.
3. P. F. BECHER and T. TIEGS, *Adv. Ceram. Mater.* **3** (1988) 148.
4. A. H. CHOKSHI and J. R. PORTER, *J. Amer. Ceram. Soc.* **68** (1985) C-144.
5. M. I. OSENDI, B. BENDER and D. LEWIS, *J. Amer. Ceram. Soc.* **72** (1989) 1049.
6. M. P. BOROM, M. K. BRUN and L. E. SZALA, *Ceram. Engng Sci. Proc.* **8** (1987) 654.
7. *Idem, Adv. Ceram. Mater.* **3** (1988) 491.
8. J. A. COSTELLO and R. E. TRESSLER, *J. Amer. Ceram. Soc.* **64** (1981) 327.
9. I. AKSAY and J. A. PASK, *ibid.* **58** (1975) 507.

Received 14 March
and accepted 30 August 1989